PROCEEDINGS OF SCIENCE

Recent results on hyperon-nucleon interactions at BESIII

Jielei Zhang[a,*]

[a] *School of Physics and Electronics, Henan University, Kaifeng 475004, People's Republic of China*

E-mail: zhangjielei@ihep.ac.cn

Hyperon-nucleon interactions are important to understand quantum chromodynamics and the so-called "hyperon puzzle" of neutron star, but limited by the availability and short-lifetime of hyperon beams, the progress of relevant research is very slow. A novel method is used to study hyperon-nucleon interactions based on hyperons produced in the decays of 10 billion J/ψ events collected with the BESIII detector at the BEPCII storage ring, being the target material is beam pipe. The reactions $\Xi^0 n \to \Xi^- p$, $\Lambda N \to \Sigma^+ X$, $\Lambda p \to \Lambda p$ and $\bar{\Lambda} p \to \bar{\Lambda} p$ have been observed and measured at BESIII. This is the first study of hyperon-nucleon interactions in electron-positron collisions and opens up a new direction for such research. Especially, antihyperon-nucleon scattering is studied for the first time.

The 11th International Workshop on Chiral Dynamics (CD2024)
26-30 August 2024
Ruhr University Bochum, Germany

*Speaker

 ISSN 1824-8039 . Published by SISSA Medialab.

PoS(CD2024)059

1. Introduction

Scattering experiments of high energy particle beams bombarding target materials have been of great significance for studying the inner structure of matter and the fundamental interactions. More than 100 years ago, Rutherford bombarded a gold foil with α particles, leading to the proposal of the atomic model [1], which opened the door for understanding the inner structure of atoms. Later, protons and neutrons as the subconstituents of the atomic nucleus were discovered [2, 3], likewise. Furthermore, different kinds of particle beams, such as $\pi^{\pm}$, $K^{\pm}$, and $p/\bar{p}$ beams, led to a series of breakthrough discoveries, like the first observation of the J/ψ charmonium and excited baryons [4, 5]. Charged long-lived particle beams such as $\pi^{\pm}/K^{\pm}$ can be easily produced in experiments. However, due to significant shorter lifetimes and higher masses, particle beams of hyperons, such as $\Lambda/\Sigma/\Xi$, are more difficult to produce experimentally and corresponding experiments are rare [5], although measurements of these beams bombarding target material are important for understanding quantum chromodynamics.

The study of hyperon-nucleon interaction is crucial for understanding the nature of neutron star (NS) [6–10], which is a gravitationally bound massive object, primarily consisting of neutrons. In the inner core of NS, it is believed that hyperons should appear because the nucleon chemical potential is large enough to make the conversion of a neutron into a hyperon energetically favorable. However, this conversion decreases the Fermi pressure of the system in the equation of state (EoS), thus, reducing the mass that NS can sustain. Many EoS calculations lead, when hyperons are present, to a maximum mass that is less than the mass of already-observed NS. This conflict is known as the "hyperon puzzle" for NS [6–10]. There have been many theoretical attempts to resolve this issue, which focus primarily on introducing a repulsive force, such as a combination of ΛN and ΛNN interactions [10–12], to help to stiffen the EoS. Therefore, more hyperon-nucleon scattering data are needed to constrain these calculations.

The hyperon-nucleon interactions have been studied by some theoretical models, including the constituent quark model [13–16], the meson-exchange picture [17, 18], and the chiral effective field theory approach [19–24]. However, the understanding of hyperon-nucleon interactions has a large uncertainty due to the lack of relevant measurements [5]. So, more experimental measurements are strongly needed to constrain the theoretical models, which can greatly promote the research in this field. Compared to the hyperon-nucleon scattering, the situation is even worse for antihyperon-nucleon scattering. Until now, no antihyperon-nucleon scattering data have been obtained due to the absence of antihyperon sources [5], which results in the very limited related theoretical research. Therefore, the realization of antihyperon-nucleon scattering measurements can fill this gap, and new measurements will motivate more effort for the understanding of the antihyperon-nucleon interaction. More importantly, antihyperon-nucleon scattering data can further constrain the hyperon-nucleon interaction theory from another angle.

The BESIII detector records symmetric e^+e^- collisions at the BEPCII collider [25]. Details of the BESIII detector can be found in Ref. [26]. With a sample of $(1.0087 \pm 0.0044) \times 10^{10}$ J/ψ events collected by the BESIII detector [27], substantial hyperons can be produced in the decays of J/ψ. The hyperons can interact with the material of the beam pipe adjacent to the e^+e^- beam, providing a novel source to study the hyperon-nucleon interactions [28, 29]. Especially, the antihyperon-nucleon interactions can also be studied using the new method. The material of the

beam pipe is composed of gold (^{197}Au), beryllium (^{9}Be) and oil (^{12}C :^{1}H= 1 : 2.13), as shown in Fig. 1. In this proceeding, the results related to the reactions $\Xi^0 n \to \Xi^- p$, $\Lambda N \to \Sigma^+ X$, $\Lambda p \to \Lambda p$ and $\bar{\Lambda} p \to \bar{\Lambda} p$ are reported [30–32], where N and X represent nucleus and anything, respectively.

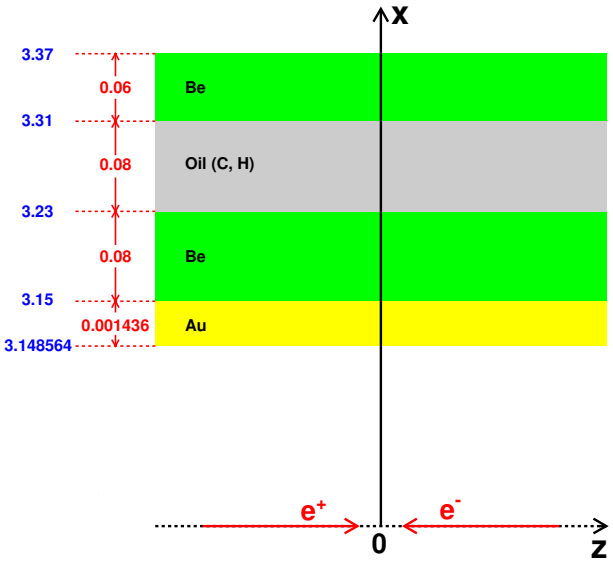

Figure 1: Schematic diagram of the beam pipe, the length units are centimeter (cm). The z-axis is the symmetry axis of the multilayer drift chamber, and the x-axis is perpendicular to the e^+e^- beam direction.

2. First study of reaction $\Xi^0 n \to \Xi^- p$ at an electron-positron collider

Using $(1.0087 \pm 0.0044) \times 10^{10}$ J/ψ events collected with the BESIII detector at the BEPCII storage ring, the process $\Xi^0 n \to \Xi^- p$ is studied, where the Ξ^0 baryon is produced in the process $J/\psi \to \Xi^0\bar{\Xi}^0$ and the neutron is a component of the ^{9}Be, ^{12}C and ^{197}Au nuclei in the beam pipe. The signal process considered in this work is $J/\psi \to \Xi^0\bar{\Xi}^0$, $\Xi^0 n \to \Xi^- p$, $\Xi^- \to \Lambda\pi^-$, $\Lambda \to p\pi^-$, $\bar{\Xi}^0 \to \bar{\Lambda}\pi^0$, $\bar{\Lambda} \to \bar{p}\pi^+$, $\pi^0 \to \gamma\gamma$, as shown in Fig. 2. The analysis method is that we use $\bar{\Xi}^0$ to tag the event and require the recoiling mass to be in the Ξ^0 mass region, then reconstruct Ξ^- and p in the signal side.

Figure 3 shows the $M(\Lambda\pi^-)$ distribution from data after final event selection, a clear Ξ^- signal is observed with a statistical significance of 7.1σ, corresponding to the reaction $\Xi^0 n \to \Xi^- p$. The cross section of the reaction $\Xi^0 + {}^{9}\mathrm{Be} \to \Xi^- + p + {}^{8}\mathrm{Be}$ is determined to be $\sigma(\Xi^0 + {}^{9}\mathrm{Be} \to \Xi^- + p + {}^{8}\mathrm{Be}) = (22.1 \pm 5.3_{\mathrm{stat}} \pm 4.5_{\mathrm{sys}})$ mb at the Ξ^0 momentum of about 0.818 GeV/c. If the effective number of reaction neutrons in a ^{9}Be nucleus is taken as 3 [33], the cross section of $\Xi^0 n \to \Xi^- p$ for a single neutron is determined to be $\sigma(\Xi^0 n \to \Xi^- p) = (7.4 \pm 1.8_{\mathrm{stat}} \pm 1.5_{\mathrm{sys}})$ mb, consistent with theoretical predictions in Refs. [15, 20, 22]. Furthermore, we do not observe any significant H-dibaryon signal in the $\Xi^- p$ final state for this reaction process [34, 35]. This work is the first study of hyperon-nucleon interactions in electron-positron collisions, and opens up a new direction for such research.

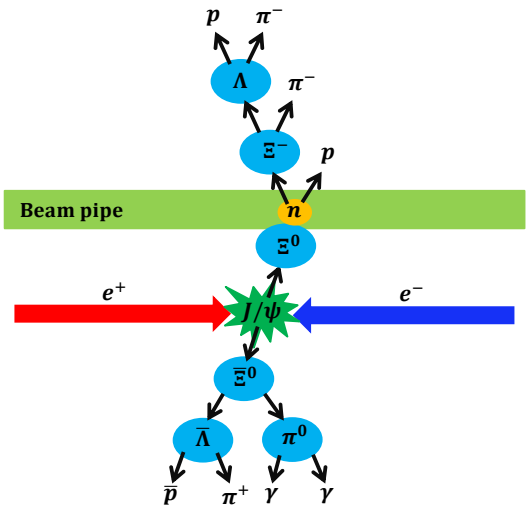

Figure 2: A complete topology diagram of the signal process $\Xi^0 n \to \Xi^- p$.

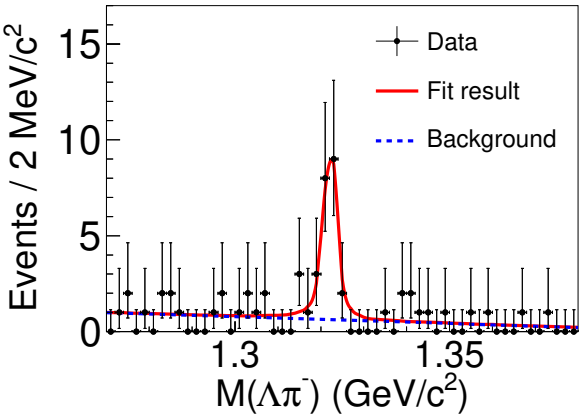

Figure 3: Distribution of $M(\Lambda\pi^-)$ in data (dots with error bars). The red solid curve is the fit result, which includes signal component and background component. The blue dashed curve is the background component.

3. First measurement of $\Lambda N \to \Sigma^+ X$ with Λ from $e^+e^- \to J/\psi \to \Lambda\bar{\Lambda}$

Using an e^+e^- collision data sample of $(1.0087\pm0.0044)\times10^{10}$ J/ψ events taken at BESIII, the process $\Lambda N \to \Sigma^+ X$ is studied for the first time. The Σ^+ hyperons are produced by the collisions of Λ hyperons from J/ψ decays with nuclei in the material of the BESIII detector. The signal process in this work is $J/\psi \to \Lambda\bar{\Lambda}$, $\Lambda N \to \Sigma^+ X$, $\Sigma^+ \to p\pi^0$, $\pi^0 \to \gamma\gamma$, $\bar{\Lambda} \to \bar{p}\pi^+$. The analysis method is that we use $\bar{\Lambda}$ to tag the event and require the recoiling mass to be in the Λ mass region, then only reconstruct Σ^+ in the signal side.

Figure 4 shows the $M_{p\pi^0}$ distribution where a clear Σ^+ signal is observed, corresponding to the reaction $\Lambda N \to \Sigma^+ X$. The total cross section of $\Lambda + {}^9\mathrm{Be} \to \Sigma^+ + X$ is measured to be $\sigma(\Lambda + {}^9\mathrm{Be} \to \Sigma^+ + X) = (37.3\pm4.7_{\mathrm{stat}}\pm3.5_{\mathrm{sys}})$ mb at the Λ momentum of about 1.074 GeV/c. Taking 1.93 as the ratio of the cross section of $\Lambda + {}^9\mathrm{Be} \to \Sigma^+ + X$ and $\Lambda p \to \Sigma^+ X$ by assuming the reaction

is dominated by the interaction of a Λ baryon with a single proton on the nucleus surface, the cross section of $\Lambda p \to \Sigma^+ X$ is determined to be $\sigma(\Lambda p \to \Sigma^+ X) = (19.3 \pm 2.4_{\rm stat} \pm 1.8_{\rm sys})$ mb. By virtue of charge independence, the cross section of $\Lambda p \to \Sigma^+ n$ is just twice that of $\Lambda p \to \Sigma^0 p$ [36], the measured result is consistent with previous experiments regarding the cross section measurements of $\Lambda p \to \Sigma^0 p$ [37]. The result will be valuable for improving the understanding of the potential of strong interaction and the origin of color confinement, as well as providing important constraints for the unified model for baryon-baryon interactions.

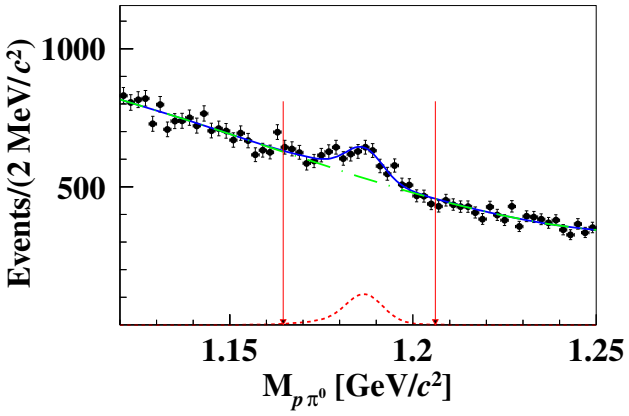

Figure 4: The $M_{p\pi^0}$ distribution with the fit result overlaid. The black dots with error bars represent the data. The blue solid line is the fit result, which includes signal component and background component. The dashed red line is the signal and the dot-dashed green line is the background. The red arrows indicate the signal range.

4. First study of antihyperon-nucleon scattering $\bar{\Lambda}p \to \bar{\Lambda}p$ and measurement of $\Lambda p \to \Lambda p$

As shown in Fig. 1, there is hydrogen in the cooling oil of the beam pipe, which are nearly static protons. Therefore, utilizing the hydrogen as the target material, the information on the (anti)hyperon-proton scattering can be extracted directly. Using $(1.0087 \pm 0.0044) \times 10^{10}$ J/ψ events, the reactions $\Lambda p \to \Lambda p$ and $\bar{\Lambda} p \to \bar{\Lambda} p$ are studied, where the $\Lambda/\bar{\Lambda}$ hyperons are produced in the process $J/\psi \to \Lambda\bar{\Lambda}$ and reconstructed via the decays $\Lambda \to p\pi^-/\bar{\Lambda} \to \bar{p}\pi^+$. The cross sections and differential cross sections of the two reactions are all measured.

For the signal reactions $\Lambda p \to \Lambda p$ and $\bar{\Lambda} p \to \bar{\Lambda} p$ produced from the decay $J/\psi \to \Lambda\bar{\Lambda}$, the momentum of the incident $\Lambda/\bar{\Lambda}$ is about 1.074 GeV/c, so the center-of-mass energy for the incident $\Lambda/\bar{\Lambda}$ and a static p is about 2.243 GeV/c^2. Figure 5 shows the $M(\Lambda p)$ and $M(\bar{\Lambda} p)$ distributions from data after the final event selection. Clear enhancement is seen around 2.243 GeV/c^2, corresponding to the reactions $\Lambda p \to \Lambda p$ and $\bar{\Lambda} p \to \bar{\Lambda} p$, respectively.

The measured differential cross sections are listed in Table 1 and shown in Fig. 6. We can see there is a slight tendency of forward scattering for $\Lambda p \to \Lambda p$, while a strong forward peak for $\bar{\Lambda} p \to \bar{\Lambda} p$ is observed. The different behaviors indicate that the reaction mechanisms of these two processes

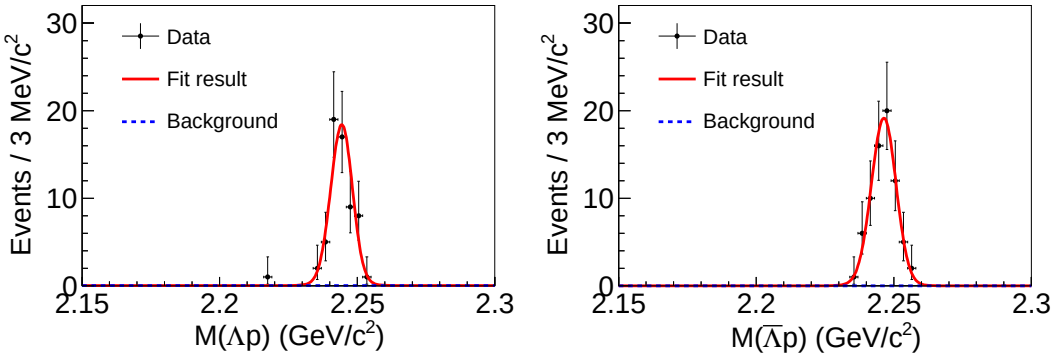

Figure 5: Distributions of $M(\Lambda p)$ (left) and $M(\bar{\Lambda}p)$ (right) of data (black dots with error bars) for the reactions $\Lambda p \to \Lambda p$ and $\bar{\Lambda}p \to \bar{\Lambda}p$, respectively. The red solid curve is the total fit result and the blue dashed curve is the background component.

are different [38, 39]. Furthermore, the cross sections in $-0.9 \leq \cos\theta_{\Lambda/\bar{\Lambda}} \leq 0.9$ are measured to be $\sigma(\Lambda p \to \Lambda p) = (12.2 \pm 1.6_{\rm stat} \pm 1.1_{\rm sys})$ mb and $\sigma(\bar{\Lambda}p \to \bar{\Lambda}p) = (17.5 \pm 2.1_{\rm stat} \pm 1.6_{\rm sys})$ mb at the $\Lambda/\bar{\Lambda}$ momentum of about 1.074 GeV/c. If we make an extrapolation for the regions of $|\cos\theta_{\Lambda/\bar{\Lambda}}| > 0.9$ for the differential cross sections of $\Lambda p \to \Lambda p$ and $\bar{\Lambda}p \to \bar{\Lambda}p$, the total elastic cross sections integrated over the full angular region are determined to be $\sigma_t(\Lambda p \to \Lambda p) = (14.2 \pm 1.8_{\rm stat} \pm 1.3_{\rm sys})$ mb and $\sigma_t(\bar{\Lambda}p \to \bar{\Lambda}p) = (27.4 \pm 3.2_{\rm stat} \pm 2.5_{\rm sys})$ mb. These constitute the first result of antihyperon-nucleon scattering, and will serve as input for the theoretical understanding of the (anti)hyperon-nucleon interaction.

Table 1: Relevant parameters for the differential cross sections, where $\cos\theta_{\Lambda/\bar{\Lambda}}$ is the scattering angle, $N_i^{\rm sig}$ is the number of signal events, ϵ_i is the efficiency, $\frac{d\sigma}{d\Omega}$ is the differential cross section, and i represents the different $\cos\theta_{\Lambda/\bar{\Lambda}}$ bins. The first value in parentheses is for $\Lambda p \to \Lambda p$, and the second for $\bar{\Lambda}p \to \bar{\Lambda}p$.

$\cos\theta_{\Lambda/\bar{\Lambda}}$	$N_i^{\rm sig}$	ϵ_i (%)	$\frac{d\sigma}{d\Omega}$ (mb/sr)
$[-0.9, -0.7]$	$(5.0^{+2.6}_{-1.9}, 0.0^{+1.1}_{-0.0})$	$(6.94, 4.93)$	$(1.7^{+0.9}_{-0.7}, 0.0^{+0.5}_{-0.0})$
$(-0.7, -0.5]$	$(1.0^{+1.4}_{-0.7}, 0.0^{+1.1}_{-0.0})$	$(14.13, 10.44)$	$(0.2^{+0.2}_{-0.1}, 0.0^{+0.3}_{-0.0})$
$(-0.5, -0.3]$	$(1.0^{+1.4}_{-0.7}, 1.0^{+1.4}_{-0.7})$	$(17.32, 13.27)$	$(0.2^{+0.2}_{-0.1}, 0.2^{+0.3}_{-0.1})$
$(-0.3, -0.1]$	$(11.0^{+3.7}_{-3.0}, 0.0^{+1.1}_{-0.0})$	$(17.74, 14.66)$	$(1.5^{+0.5}_{-0.4}, 0.0^{+0.2}_{-0.0})$
$(-0.1, 0.1]$	$(6.9^{+3.0}_{-2.3}, 0.0^{+1.1}_{-0.0})$	$(19.11, 15.79)$	$(0.9^{+0.4}_{-0.3}, 0.0^{+0.2}_{-0.0})$
$(0.1, 0.3]$	$(5.0^{+2.6}_{-1.9}, 2.0^{+1.8}_{-1.1})$	$(19.53, 16.82)$	$(0.6^{+0.3}_{-0.2}, 0.3^{+0.3}_{-0.2})$
$(0.3, 0.5]$	$(12.0^{+3.8}_{-3.1}, 7.0^{+3.0}_{-2.3})$	$(19.21, 17.68)$	$(1.5^{+0.5}_{-0.4}, 1.0^{+0.4}_{-0.3})$
$(0.5, 0.7]$	$(13.0^{+3.9}_{-3.3}, 25.0^{+5.3}_{-4.7})$	$(19.71, 17.60)$	$(1.6^{+0.5}_{-0.4}, 3.4^{+0.7}_{-0.6})$
$(0.7, 0.9]$	$(6.0^{+2.8}_{-2.1}, 37.0^{+6.4}_{-5.8})$	$(9.80, 9.93)$	$(1.5^{+0.7}_{-0.5}, 9.0^{+1.6}_{-1.4})$

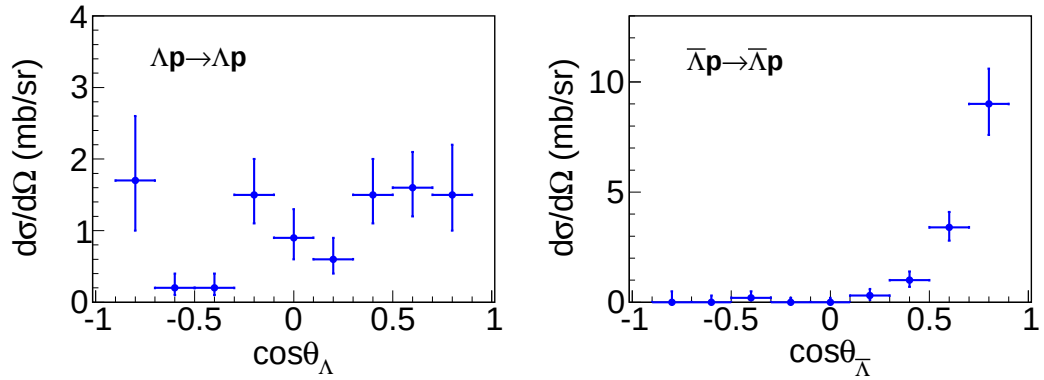

Figure 6: Differential cross sections of the reactions $\Lambda p \to \Lambda p$ (left) and $\bar{\Lambda} p \to \bar{\Lambda} p$ (right) for the $\Lambda/\bar{\Lambda}$ momentum of around 1.074 GeV/c.

5. Summary

In summary, the hyperon-nucleon interactions are studied using a novel method at BESIII. The hyperons are produced in the decays of J/ψ events and the beam pipe acts as the target material. The reactions $\Xi^0 n \to \Xi^- p$, $\Lambda N \to \Sigma^+ X$, $\Lambda p \to \Lambda p$ and $\bar{\Lambda} p \to \bar{\Lambda} p$ are observed and measured at BESIII [30–32]. These new results enhance the understanding of hyperon-nucleon interactions and further help to understand baryon-baryon interactions in a unified perspective. This first study of hyperon-nucleon interactions in electron-positron collisions opens up a new direction for such research. Especially, antihyperon-nucleon scattering is studied for the first time.

Using the same method, other (anti)hyperon-nucleon reactions can also be studied at BESIII, so more interesting results will come out soon. Furthermore, we may be able to design targets of specific materials to study (anti)hyperon-nucleon interactions in future super tau-charm facilities [40, 41]. With more statistics at that time, we can also study the momentum-dependent cross section or differential cross section distributions based on the (anti)hyperons from multi-body decays of J/ψ or other charmonia.

Acknowledgments

This work is supported by Natural Science Foundation of Henan under Contract No. 242300421163 and National Natural Science Foundation of China (NSFC) under Contract No. 12375071.

References

[1] E. Rutherford, Phil. Mag. Ser. 6 **21**, 669 (1911).

[2] E. Rutherford, Phil. Mag. Ser. 6 **37**, 581 (1919).

[3] J. Chadwick, Nature **129**, 312 (1932).

[4] J. J. Aubert *et al.* [E598 Collaboration], Phys. Rev. Lett. **33**, 1404 (1974).

[5] S. Navas *et al.* [Particle Data Group], Phys. Rev. D **110**, 030001 (2024).

[6] I. Vidaña, Nucl. Phys. A **914**, 367 (2013).

[7] D. Chatterjee and I. Vidaña, Eur. Phys. J. A **52**, 29 (2016).

[8] I. Vidaña, Proc. Roy. Soc. Lond. A **474**, 0145 (2018).

[9] Z. Q. Feng, Phys. Lett. B **851**, 138580 (2024).

[10] L. Tolos and L. Fabbietti, Prog. Part. Nucl. Phys. **112**, 103770 (2020).

[11] D. Lonardoni, A. Lovato, S. Gandolfi and F. Pederiva, Phys. Rev. Lett. **114**, 092301 (2015).

[12] J. Haidenbauer, U. G. Meißner and A. Nogga, Eur. Phys. J. A **56**, 91 (2020).

[13] C. Nakamoto, Y. Fujiwara and Y. Suzuki, Nucl. Phys. A **639**, 51 (1998).

[14] V. G. J. Stoks and T. A. Rijken, Phys. Rev. C **59**, 3009 (1999).

[15] Y. Fujiwara, M. Kohno, C. Nakamoto and Y. Suzuki, Phys. Rev. C **64**, 054001 (2001).

[16] Q. Liu and I. Low, Phys. Lett. B **856**, 138899 (2024).

[17] M. Yamaguchi, K. Tominaga, T. Ueda and Y. Yamamoto, Prog. Theor. Phys. **105**, 627 (2001).

[18] J. Haidenbauer and U. G. Meißner, Phys. Rev. C **72**, 044005 (2005).

[19] H. Polinder, J. Haidenbauer and U. G. Meißner, Phys. Lett. B **653**, 29 (2007).

[20] J. Haidenbauer, U. G. Meißner and S. Petschauer, Nucl. Phys. A **954**, 273 (2016).

[21] K. W. Li, X. L. Ren, L. S. Geng and B. W. Long, Chin. Phys. C **42**, 014105 (2018).

[22] J. Haidenbauer and U. G. Meißner, Eur. Phys. J. A **55**, 23 (2019).

[23] J. Song, Z. W. Liu, K. W. Li and L. S. Geng, Phys. Rev. C **105**, 035203 (2022).

[24] R. Y. Zheng, Z. W. Liu, L. S. Geng, J. N. Hu and S. Wang, Phys. Lett. B **864**, 139416 (2025).

[25] C. H. Yu *et al.*, Proceedings of IPAC2016, Busan, Korea, 2016, doi:10.18429/JACoW-IPAC2016-TUYA01.

[26] M. Ablikim *et al.* [BESIII Collaboration], Nucl. Instrum. Meth. A **614**, 345 (2010).

[27] M. Ablikim *et al.* [BESIII Collaboration], Chin. Phys. C **46**, 074001 (2022).

[28] C. Z. Yuan and M. Karliner, Phys. Rev. Lett. **127**, 012003 (2021).

[29] J. P. Dai, H. B. Li, H. Miao and J. Y. Zhang, Chin. Phys. C **48**, 073003 (2024).

[30] M. Ablikim *et al.* [BESIII Collaboration], Phys. Rev. Lett. **130**, 251902 (2023).

[31] M. Ablikim *et al.* [BESIII Collaboration], Phys. Rev. C **109**, L052201 (2024).

[32] M. Ablikim *et al.* [BESIII Collaboration], Phys. Rev. Lett. **132**, 231902 (2024).

[33] J. K. Ahn, S. Aoki, K. S. Chung, M. S. Chung, H. En'yo, T. Fukuda, H. Funahashi, Y. Goto, A. Higashi and M. Ieiri, *et al.* Phys. Lett. B **633**, 214 (2006).

[34] R. L. Jaffe, Phys. Rev. Lett. **38**, 195 (1977).

[35] A. T. M. Aerts, P. J. G. Mulders and J. J. de Swart, Phys. Rev. D **17**, 260 (1978).

[36] J. A. Kadyk, G. Alexander, J. H. Chan, P. Gaposchkin and G. H. Trilling, Nucl. Phys. B **27**, 13 (1971).

[37] J. M. Hauptman, J. A. Kadyk and G. H. Trilling, Nucl. Phys. B **125**, 29 (1977).

[38] J. Haidenbauer and U. G. Meißner, Eur. Phys. J. A **60**, 119 (2024).

[39] X. Y. Wang, Y. Gao and X. Liu, Phys. Lett. B **862**, 139321 (2025).

[40] A. E. Bondar *et al.* [Charm-Tau Factory Collaboration], Phys. Atom. Nucl. **76**, 1072 (2013).

[41] M. Achasov *et al.*, Front. Phys. **19**, 14701 (2024).